Journal of Materials Chemistry A

Accepted Manuscript

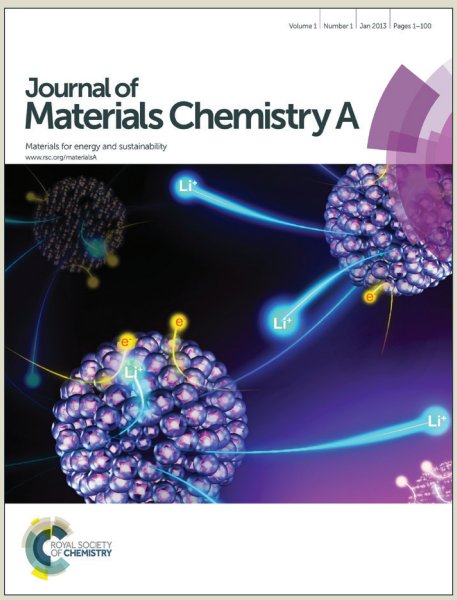

ROYAL SOCIETY OF CHEMISTRY

www.rsc.org/materialsA

Cite this: DOI: 10.1039/c0xx00000x

www.rsc.org/xxxxxx

ARTICLE TYPE

Investigation of cyano resin based gel polymer electrolyte: in-situ gelation mechanism and electrode/electrolyte interfacial fabrication in lithium-ion battery †

Dong Zhou,‡[a,b] Yan-Bing He,‡[a] Qiang Cai,[b] Xianying Qin,[a] Baohua Li,[a] Hongda Du,[a] Quan-Hong Yang[a] and Feiyu Kang[a,b]*

Received (in XXX, XXX) Xth XXXXXXXXX 20XX, Accepted Xth XXXXXXXXX 20XX
DOI: 10.1039/b000000x

Cyanoethyl polyvinyl alcohol (PVA-CN) based gel polymer electrolyte (GPE) is a high performance electrolyte for lithium-ion batteries (LIBs), which is in-situ synthesized by stable monomer without using additional initiators. Unfortunately, the gelation mechanism of PVA-CN is still unclear. Furthermore, for general GPEs prepared by in-situ polymerization, the electrode/GPE interface in batteries remains to be further optimized. Here we present the gelation mechanism of the PVA-CN based GPE and fabricate an electrode/GPE interface with less resistance during battery formation. The cross-linkable PVA-CN based organogel is formed via in-situ cationic polymerization of the cyano resin initiated by PF_5, a strong lewis acid produced by the thermo-decomposition of $LiPF_6$. It is interesting to find that the battery formation process completed in the precursor solution instead of in the gel can greatly reduce the interfacial resistance of graphite/GPE and benefit the formation of a more stable solid electrolyte interface (SEI) on anode, which contribute to a dramatic improvement of battery performance. This work gives an useful guidance towards designing new GPE materials and promoting their practical application in LIBs.

Lithium-ion batteries (LIBs) are the current hottest energy storage devices for portable device, electric vehicle and bulk electricity storage at power stations, since they are characterized by high energy density, high working voltage, long life, environmentally friendly operation and memory-effect-free[1, 2]. However, one of the biggest obstacles for the further development of high capacity and high power LIBs is safety issues such as fire, explosion and electrolyte leakage caused by the flammable organic electrolyte. Efficient electrolyte materials are the hard core for the security assurance and cyclicity improvement of LIBs[3, 4]. Among the potential electrolyte types for LIBs, gel polymer electrolyte (GPE) has been given extensive attention due to its high ionic conductivity, superior electrochemical performance, flexible processability and no liquid electrolyte leakage[5, 6].

In recent years, in-situ synthesis, which completes the preparation of GPEs and the formation of polymer LIBs in one step, has been a hot area in the preparation of GPEs. In this process, the initiators, cross-linkers and monomers (such as acrylic esters[7-9], ethylene oxide[10]) are dissolved in a liquid electrolyte to form a precursor solution, which is injected into the battery package and absorbed into the separator. And then a free radical polymerization[11, 12] or ionic polymerization[13] of monomers are triggered by thermal initiation[14, 15], ultraviolet ray (UV)[16] or γ-ray irradiation[17] in the presence of liquid electrolyte solvent. The obtained GPEs, consisting of a cross-linked polymer network filled with a high content of liquid electrolyte, have a satisfactory ionic conductivity as well as a good contact and affinity with the electrodes[18]. This synthesis technology provides a simple scheme to prepare the GPEs with high performance and also greatly simplifies the assembly process of polymer LIBs. However, the polymerization reaction of monomers heavily relies on the initiators. It is well-known that both the monomers and initiators have high reactivity. The initiator can also promote an adverse polymerization of the solid electrolyte interface (SEI) forming additives featured by C=C bonds in their molecules, such as vinylene carbonate (VC). The consumption of SEI forming additives reduces the stability of SEI film and causes an increase of irreversible capacity and a reduction of cycling performance[19]. In addition, the monomers tend to self-polymerize meanwhile the initiation activity of initiators is easily lost during storage at room temperature, which reduces the uniformity of full batteries and introduces difficulties in large scale commercial application of

[a] *Engineering Laboratory for the Next Generation Power and Energy Storage Batteries, and Engineering Laboratory for Functionalized Carbon Materials, Graduate School at Shenzhen, Tsinghua University, Shenzhen 518055, China, fykang@mail.tsinghua.edu.cn*
[b] *Laboratory of Advanced Materials, School of Materials Science and Engineering, Tsinghua University, Beijing 100084, China*
† *Electronic supplementary information (ESI) available: Schematic representation of the separation and purification of the polymer matrix from GPEs; Optical images of PVA-CN sample and PVA-CN based GPE battery; Experimental and simulation EIS curves of a polymer LIB. See DOI:*
‡ *These two authors are equal main contributors.*

in-situ synthesis of GPEs. Therefore, finding an optimized polymerization system with stable monomers and initiator-free is of great significance to the industrial development of polymer LIBs.

Recently, a new type monomer of cyanoethyl polyvinyl alcohol (PVA-CN) was reported to prepare GPEs by an in-situ heating process in a 1 M $LiPF_6$ liquid electrolyte solution without any additional initiators or cross-linkers, which exhibits a high Li^+ transference number (> 0.84), a high ionic conductivity close to liquid electrolytes, and an excellent capacity retention and thermal stability in LIBs[20]. These GPEs may have a great application promise in the polymer LIBs. The authors speculated the gelation mechanism of PVA-CN that was a thermally initiated physical process induced by entropic gain of Gibbs free energy[20].

However, in this work, a totally different gelation mechanism of PVA-CN was found based on the systematic experimental results. The gelation process of PVA-CN is not a physical process, but a chemical reaction. The PVA-CN based organogel was formed via in-situ cationic polymerization of the cyano resin initiated by PF_5 as a strong lewis acid produced by the thermo-decomposition of $LiPF_6$. To the best of our knowledge, this cationic polymerization of the cyano group is unreported in previous researches on GPEs. In addition, for general GPEs prepared by in-situ polymerization, the battery formation process may play a key role in the fabrication of electrode/GPE interface, since SEI film is formed and organic gases are generated during this process[21, 22]. Here a better electrode/electrolyte interface with less resistance is fabricated by optimizing the battery formation process. The interfacial resistance of LIBs with the GPEs gelled after battery formation is much less than that of GPEs gelled before formation, which results in a better performance of the former LIBs.

Experimental

Synthesis of PVA-CN based GPE

GPE was prepared by in-situ gelation of a precursor solution in a sealed transparent glass container. The precursor solution was composed of 2 wt.% PVA-CN (Shin-Etsu Chemical, **Fig. S1**a) dissolved in a liquid electrolyte consisted of 1M $LiPF_6$ in a non-aqueous solution of ethylene carbonate (EC)/ dimethyl carbonate (DMC)/ ethylmethyl carbonate (EMC) with a volume ratio of 1:1:1. The contents of trace water in liquid electrolyte and precursor solution were detected by Karl Fisher method (831 KF Coulometer, Metrohm). The precursor solution was heated at a temperature of 70 ^oC to obtain black PVA-CN based GPE (**Fig. S1**b). All the reagents were of battery grade and used without further purification, and all procedures for preparing the GPE were carried out in an Ar-filled glove box. This synthesis route is displayed in **Fig. S2**.

Separation and purification of the polymer matrix from GPEs

A schematic representation illustrating the operational process of the separation and purification of the polymer matrix from GPEs is provided in **Fig. S2**. The GPEs were mashed into pieces and washed with acetone, and then the mixture was centrifuged at 10,000 rpm for 15 minutes to separate the black precipitates. Above procedures were repeated three times followed by a vacuum drying at 120 ^oC. The obtained black precipitates were dialyzed against deionized water for 3 days to further remove the residual ion and then the precipitates were vacuum dried at 120 ^oC again to obtain the separated PVA-CN based polymer matrix.

The microstructure and spectral characterization of the polymer matrix

The microstructure of the polymer matrix was characterized with field emission scanning electron microscopy (FE-SEM, HITACH S4800) at 10 kV. In-situ monitoring of the reaction of precursor solution during the heating process was taken using an ultraviolet and visible spectrum (UV/VIS, Shimadzu UV-2450). The fourier transform infrared (FTIR) spectrum of the PVA-CN resins and the prepared polymer matrixes were recorded with a Bruker Vertex70 instrument at ambient temperature. X-ray photoelectron spectroscopy (XPS) measurements were conducted on a Physical Electronics PHI5802 instrument using an X-rays magnesium anode (monochromatic Ka X-rays at 1253.6 eV) as the source. C 1s region were used as references and set at 284.8 eV.

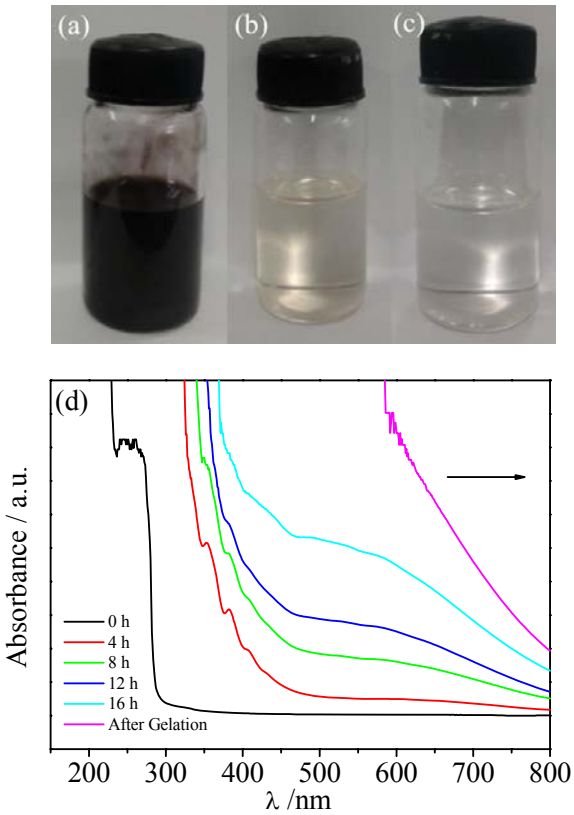

Figure 1. Reaction rules of PVA-CN in electrolyte solvents: optical images of the solution of 2 wt.% PVA-CN dissolved in 1M $LiPF_6$/ EC:DMC:EMC (a), 1M $LiClO_4$/ EC:DMC:EMC (b) and pure EC:DMC:EMC solvent (c) heated at 70 ^oC for 24 h; UV/VIS spectroscopic monitoring of the reaction of 2 wt.% PVA-CN dissolved in 1M $LiPF_6$/ EC:DMC:EMC liquid electrolyte heated at 70 ^oC for different reaction times (d).

Preparation and electrochemical characterization of PVA-CN based GPE batteries

Commercial 034352 type graphite/$LiCoO_2$ batteries were assembled with a capacity of 2100 mAh. These batteries were made of $LiCoO_2$ as the cathode, graphite as the anode, polyethylene as the separator, and precursor solution (2 wt.% PVA-CN dissolved in 1M $LiPF_6$/ EC:DMC:EMC liquid electrolyte) as the electrolyte. The cathodes were prepared by mixing 95 wt.% $LiCoO_2$ with 2 wt.% carbon black (Super-P) and 3 wt.% polyvinylidene fluoride (PVDF), while the anodes were prepared by mixing 97.5 wt.% graphite with 1.5 wt.%

styrene-butadiene rubber (SBR) and 1 wt.% carboxy-methyl cellulose (CMC). These components were rolled together to form the battery core and assembled into aluminum-plastic laminated film packages (**Fig. S1**c), followed by injecting the precursor solution into the packages and sealing batteries under vacuum. After that, the assembled cells were aged at room temperature for 12 hours to ensure the precursor solution well wetted into the electrodes, and then treated with following two different processing technologies:

Technology 1: Firstly, the assembled batteries were baked at 70 °C under 0.25 MPa for 24 h to make the precursor solution adequately transform into GPEs, and then batteries were subjected to a formation process (galvanostatically charged at 0.05 C for 2 hours followed by charged at 0.1 C for 5 hours). Finally, batteries were aged at 25° C for 12 h and degassed. An optical image of finished battery is shown in **Fig. S1**d.

Technology 2: Firstly, the assembled batteries were subjected to a formation process same as Technology 1, and then the batteries were baked at 70 °C under 0.25 MPa for 24 h. Finally, the batteries were aged at 25 °C for 12 h and degassed.

Charge-discharge tests of PVA-CN based GPE batteries were carried out at 0.2 C using a LAND-CT2001A cell test instrument at 25 °C. During each test cycle, the batteries were galvanostatically charged to 4.35 V and then potentiostatically charged at 4.35 V until the current dropped to 21 mA (0.01 C) and then discharged to 3 V at 0.2 C. The EIS was measured to investigate the interfacial behavior of the assembled cells, using an electric IM6ex impedance analyzer in the frequency range of 10^{-2} to 10^{5} Hz. The EIS of batteries were measured at 4.0 V by applying a 5 mV ac oscillation.

Cyclic voltammograms (CV) were recorded with a VMP3 multichannel electrochemical station at a scan rate of 0.1 mV s^{-1} in the range of 2.5-4.4 V using CR2032 type $LiCoO_2$|GPE|graphite coin cells. The compositions of electrodes and precursor solution were same as the 034352 type batteries. For Technology 1, cells injected with precursor solution were firstly baked at 70 °C for 24h and then tested 5 CV cycles; For Technology 2, cells were performed 2 cycles CV test followed by a heating process at 70 °C for 24h, and then further subjected to another 3 CV cycles.

Results and Discussion

Investigation of the in-situ gelation mechanism

To identify the initiation system of the gel reaction, 2 wt. % PVA-CN resin were dissolved in 1M $LiPF_6$/ ethylene carbonate (EC): dimethyl carbonate (DMC): ethylmethyl carbonate (EMC), 1M $LiClO_4$/EC:DMC:EMC and pure EC:DMC:EMC solvent, respectively, and then above solutions were heated at 70 °C for 24 hours. Interestingly, the black GPEs were only formed in presence of $LiPF_6$, while no gelation could be observed in 1M $LiClO_4$/EC:DMC:EMC or pure EC:DMC:EMC solvent, as shown in **Fig. 1**a-c. It is exhibited that the PF_6^- plays a key role in the gel reaction of PVA-CN.

Ultraviolet and visible spectrum (UV/VIS) is used to in-situ monitor the reaction of PVA-CN in 1M $LiPF_6$ / EC:DMC:EMC liquid electrolyte during the heating process. In **Fig**. **1**d, the initial precursor solution has a strong absorption in the UV region, which gradually shifts to the visible region with the prolongation of the reaction time. Similar absorption patterns could be observed in the polymerization reactions of fumarocyano[23]. The result indicates that a conjugated π-system was formed[24] and some polymerization reaction occurred in the gelation process.

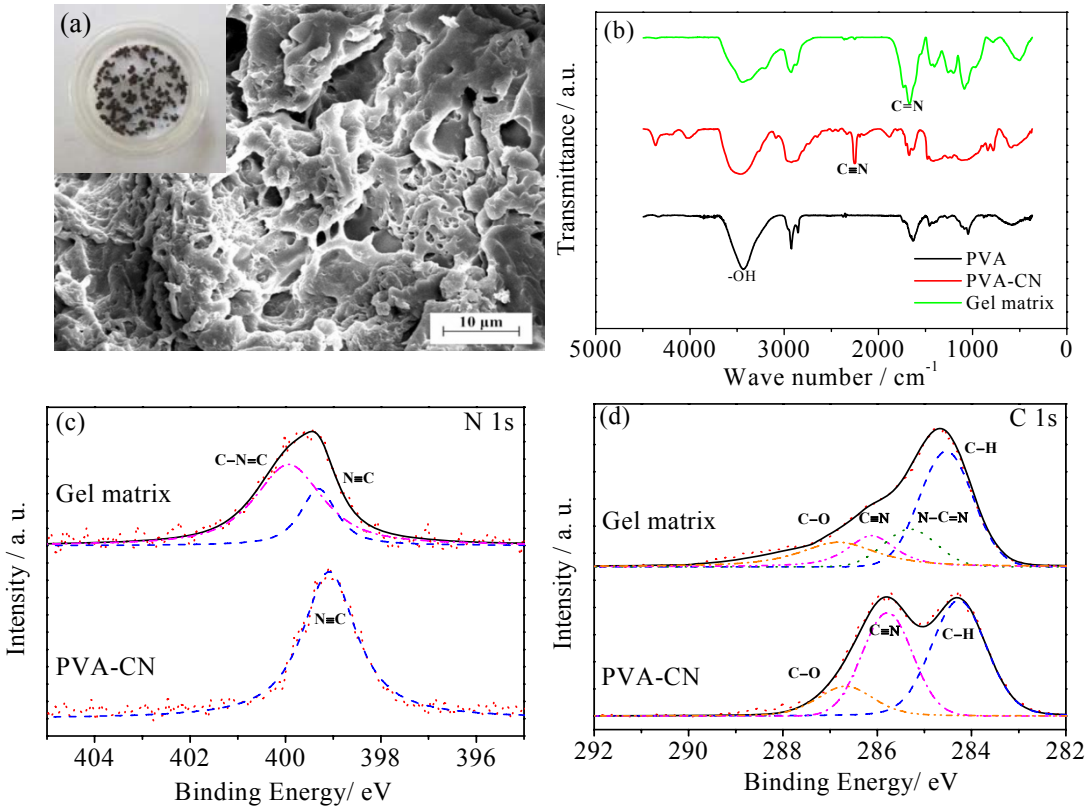

Fig. 2. Characterization of the polymer matrixes in PVA-CN based GPEs: optical and FE-SEM images of the polymer matrixes (a); FTIR spectra (b), XPS spectra of N1s (c) and C1s (d) for PVA-CN and the polymer matrix.

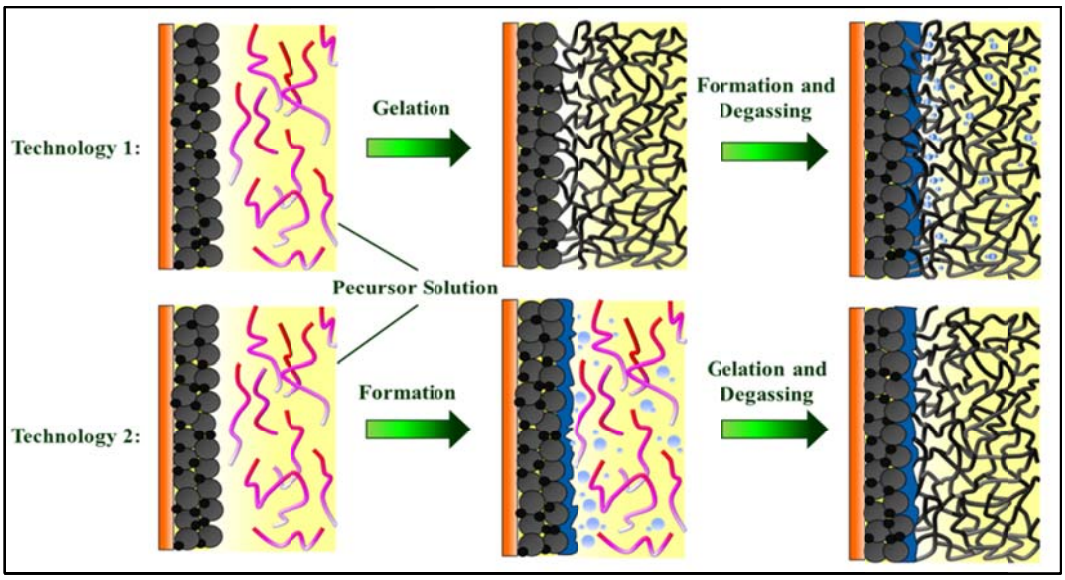

Fig. 4. Schematic illustration for the gelation and formation of PVA-CN based polymer LIBs with different formation technologies.

To further identify the reactive groups in PVA-CN molecules, the polymer matrix was separated and purified from PVA-CN based GPEs. Typical optical and field emission scanning electron microscopy (FE-SEM) images in **Fig. 2**a present that the obtained polymer matrix is an obviously porous network polymer. In GPEs, this polymer matrix acting as internal scaffolding is well cross-linked to establish a three-dimensional framework with high porosity, and liquid electrolyte can be highly dispersed in this polymer framework. **Fig. 2**b gives the fourier transform infrared spectra (FTIR) for pure PVA (polyvinyl alcohol), PVA-CN and the polymer matrix of GPEs to infer the gelation mechanism. As can be seen, the appearance of the C≡N bonds at 2250 cm^{-1} and the intensity decrease of OH bond at 3432–3461 cm^{-1} in the FTIR spectrum of PVA-CN indicates that the OH groups in PVA are converted to OCH_2CH_2CN groups in the cyanoethylation of PVA[25]. The FTIR spectrum of the polymer matrix shows that the absorption peak at around 2250 cm^{-1} belonged to C≡N bonds almost disappears, while the intensity of peak at 1670 cm^{-1} apparently increases, indicating the presence of C=N bonds in the polymer matrix[26]. The result of FTIR spectrum demonstrates that the C≡N bonds were cloven in the gelation reactions of PVA-CN and a new conjugated structure with C=N bonds was formed.

The X-ray photoelectron spectra (XPS, C 1s and N 1s) further support the polymerization of the cyano group. As shown in **Fig. 2**c, the N 1s spectrum for PVA-CN shows a single symmetrical peak appeared at 399.2 eV, belonged to C≡N bonds[27]. However, the N 1s spectrum for polymer matrix of GPEs shows a asymmetric peak shifting to high binding energy, which can be fitted into two sub-peaks, assigned to C-N=C and C ≡ N, respectively[28]. The C 1s spectra for PVA-CN and the polymer matrix of GPEs are given in **Fig. 2**d, which can be decomposed into four sub-peaks appeared at 284.6, 285.0, 286.3, and 286.4 eV assigned to C-H, N-C=N, C≡N and C-O, respectively[29-31]. As can be seen from the C 1s spectrum for the polymer matrix of GPEs, the intensity of the peak belonged to C≡N apparently decreases while an obvious new peak assigned to N-C=N appears, indicating a polymerization reaction of the cyano group occurs in the process of gelation that is consistent with the results of N 1s and FTIR spectra (**Fig. 2**b).

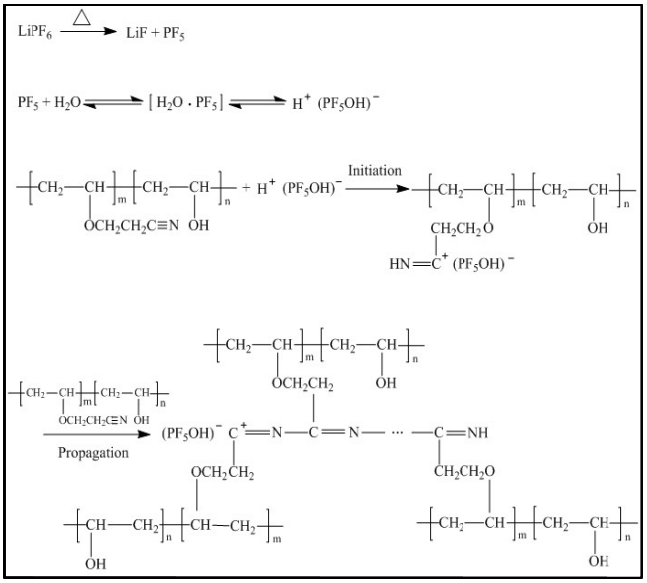

Fig. 3. Polymerization mechanism of PVA-CN in electrolyte solvents.

On the bases of the experimental results stated above, the reaction mechanism of PVA-CN in-situ gelation can be deduced as a cationic polymerization of cyano group initiated by PF_5, a strong lewis acid produced by the thermo-decomposition of $LiPF_6$ under heating conditions[21]. These macromolecule chemical reactions are expressed in **Fig. 3**. PF_5 as a common cationic polymerization initiator can react with the trace water in the precursor solution of GPEs (tested to be 14.6 ppm by Karl Fisher method) as a Lewis base to form $H^+(PF_5OH)^-$[32], which acts as an initiating system to promote the gelation reaction. During the initiation of the reaction, $H^+(PF_5OH)^-$ attacks the cyano group and generates the carbenium ions. The propagation proceeds via the impregnation of PVA-CN monomer to these carbenium ions,

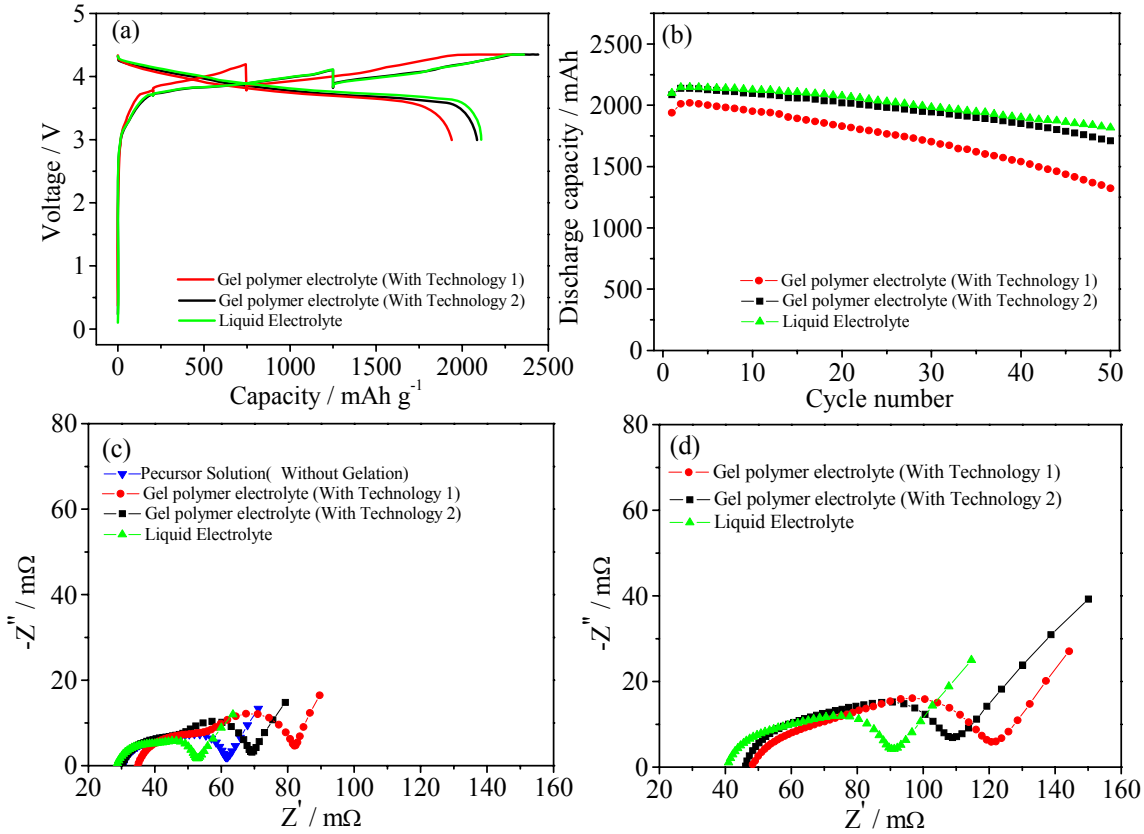

Fig. 5. Initial charge and discharge curves (a) and cycling performance (b) of PVA-CN based polymer LIBs with different processing technologies at 0.2C; EIS of the PVA-CN based polymer LIBs with different formation technologies after 1 cycle (c) and 50 cycles (d) at 0.2 C. Impedances are measured at half state of the charge (4.0 V).

finally giving rise to a cross-linked three-dimensional network structure filled by liquid electrolyte and forming GPEs[33]. So far, few studies have explored the polymerization of nitriles because C≡N bonds are inherently stable and the enthalpy of this polymerization is small while the entropy change of this reaction is a negative value, resulting in an increase of the Gibbs free energy[34]. However, in this work, the polymerization of C≡N can be successfully initiated by the PF_5 and this reaction mechanism provides a new way for the design and preparation of cyano electrolyte materials.

Fabrication of electrode/electrolyte interface with low resistance

At present, for general GPEs prepared by in-situ polymerization, the effect of the battery formation process on the fabrication of electrode/GPE interface remains unclear. Here, the soft-packed graphite/$LiCoO_2$ batteries using PVA-CN based GPEs with a designed capacity of 2100 mAh were prepared to investigate and optimize the electrode/GPE interface during formation process. Two type formation technologies based on the gelation sequence were designed as shown in experimental and **Fig. 4** (Technology 1: gelation before battery formation; Technology 2: gelation after battery formation). To better investigate the effects of the different formation technologies on the battery performance, no additives are added into the liquid electrolyte to reduce the gas generation, which makes the contrast more remarkable.

Fig. 5a shows the initial charge and discharge curves of $LiCoO_2$|GPE|graphite cells at a rate of 0.2 C using two type formation technologies. It is noteworthy that the formation technology has great influence on the formation voltage of batteries. The voltage of battery using Technology 1 rapidly increases to the cut-off voltage of 4.35V, whereas that using Technology 2 increases gradually, similar to that of liquid electrolyte battery. This phenomenon can be interpreted as followed. It is well-known that the SEI film is formed on the surface of graphite anode along with a generation of organic gases during the formation process of battery[21, 22]. When the PVA-CN is gelled before battery formation (Technology 1), a layer of formed PVA-CN based gel is covered on the surface of graphite (**Fig. 4**), which hinders the reduction of liquid electrolyte. A poor SEI with high resistance will be formed on the interface between GPE and graphite that leads to a larger polarization during battery formation. Furthermore, the battery formation process is completed in quasi-solid phase. Myriad of tiny bubbles were formed and accumulated on the surface of electrode because the diffusion of bubbles in the gel is much slower than that in the liquid electrolyte solution (from the electrode surface to the gasbag), as schematically illustrated in **Fig. 4**. These bubbles hinder the intercalation of lithium ion and lead to a large ion concentration polarization, which result in a rapid rise of interface voltage. Whereas, when the battery is subjected to the formation before gelation of PVA-CN (Technology 2), PVA-CN based gel is covered on the formed SEI with lower resistance and nearly no bubbles were accumulated on the surface of electrode (**Fig. 4**). This interface structure can be expected to have high electrochemical stability and less polarization. After formation and gelation, the batteries were degassed. It is seen that the

charge voltage of battery using Technology 1 is obviously higher than that of batteries using liquid electrolyte and Technology 2, indicating that the polarization of former battery is much larger than that of latter batteries.

An initial reversible capacity of 2086 mAh and a coulombic efficiency of 85.5% are observed when the GPE type batteries were treated with Technology 2, which are much closer to that of batteries using liquid electrolyte (2111 mAh and 89.5%). Whereas the batteries with Technology 1 can only deliver the capacity of 1939 mAh and a coulombic efficiency of 84.9%. It is seen that the formation technology has a remarkable influence on the reversible capacity of PVA-CN based battery. The cycling performance of GPE type batteries are shown in **Fig. 5**b. The capacity retention ratio are 82.0 and 86.0% for the GPE type battery with Technology 2 and battery using liquid electrolyte after 50 cycles at 0.2 C, respectively. This slight difference in cycling performance can be explained as the side reaction of the unreacted monomer at the electrode surface, which forms a resistive film and increases the interfacial resistance[35]. In contrast, the GPE type battery with technology 1 only exhibits a capacity retention ratio of 68.2% after 50 cycles at 0.2 C, which is much lower than that technology 2. The charge and discharge curves of PVA-CN based polymer LIBs at 0.2C for some selected cycle numbers are shown in **Fig. S4**. Evidently, the charge/discharge potential gap of battery with Technology 2 is much less than that of battery with Technology 1. The lower potential gap implies a lower polarization and interfacial resistance during cycling. The above results fully exhibit that the battery formation before gelation of PVA-CN benefits the electrochemical performance of GPE type batteries.

Electrochemical impedance spectrum (EIS) is used to evaluate the interfacial behavior and reversibility of PVA-CN based polymer LIBs. The EIS of $LiCoO_2$|GPE|graphite batteries with different formation technologies after 1 cycle and 50 cycles are shown in **Fig. 5**c and d, which are composed of two partially overlapped and depressed semicircles at high to middle frequency and a slope line at low frequency[36-39]. The spectra are simulated by Z-view software using an equivalent circuit shown in **Fig. S3**[40], while the values of impedance parameters are listed in **Tables 1**. As can be seen from **Fig. S3**, the experimental and simulation spectra are almost coincident. According to the equivalent circuit, the intersection of the diagram with real axis refers to a bulk resistance (R_b), mainly reflecting the resistance of electrodes and electrolyte/separator. The depressed semicircle at high frequency can be attributed to the resistance of SEI (R_{SEI}) and CPE1, while the depressed semicircle at medium frequency can be attributed to the charge transfer resistance (R_{ct}) and CPE2. Instead of the capacitance of the SEI (C_{SEI}) and double-layer capacitance (C_{dl}), CPE1 and CPE2 are the constant phase elements used to take into account the roughness of the particle surface. The slope line at low frequency is equivalent to the Warburg impedance (Z_w), which is related to the lithium ion diffusion within the particles[39].

The simulation results in **Table 1** present that the R_b and R_{ct} of batteries using PVA-CN precursor solution without gelation have a minor increase in comparison with the batteries using liquid electrolyte, which is attributed to a decrease in the electrolyte conductivity caused by the increase in electrolyte viscosity[20]. When the PVA-CN precursor solution was converted into GPE after battery formation (Technology 2), the R_b and R_{ct} of batteries have no significant changes and the R_{SEI} has a notable increase, suggesting that gel matrixes with high resistivity grow on the surface of SEI. However, when the PVA-CN is gelled before the battery formation (Technology 1), the R_b and R_{SEI} of battery have a dramatic increase compared to batteries with Technology 2, which can be attributed to two factors: firstly, a pre-covered layer of PVA-CN gel matrixes was formed on the electrode surface before the battery formation process, which leads to the construction of a poor SEI with high resistance as mentioned above; secondly, the generated residual bubbles during formation are difficult to exhaust through the framework structure of gel via degassing, which would linger in the GPE and blocks the transformation of lithium ions. These increases in R_b and R_{SEI} may result in a reduction in initial capacity.

After 50 cycles, the increase of R_b, R_{ct} and R_{SEI} for battery using formation Technology 1 is much larger than that of battery using formation Technology 2, especially for the values of R_b and R_{ct}, which indicates that the former battery system is not stable due to its poor SEI film on the graphite and high resistance interface between GPE and graphite anode. The electrolyte consumption, deterioration contacts and undesirable side reactions between the electrolyte and electrode was promoted in this battery[41, 42]. Furthermore, the dendrite Li may be formed on the negative electrode resulted from the uneven current density distribution caused by the residual bubbles[43]. Therefore, the capacity of battery using formation Technology 1 rapidly fade during battery cycling tests as shown in **Fig. 5**b.

Table 1 Simulation results of **Fig. 5**.

	After 1 cycle			After 50 cycles		
	R_b (mΩ)	R_{SEI} (mΩ)	R_{ct} (mΩ)	R_b (mΩ)	R_{SEI} (mΩ)	R_{ct} (mΩ)
Precursor Solution （Without Gelation）	31.19	10.52	19.27	/	/	/
Gel polymer electrolyte (With Technology 1)	34.96	23.61	23.06	54.59	29.07	48.58
Gel polymer electrolyte (With Technology 2)	31.43	16.89	21.28	45.62	20.59	37.48
Liquid Electrolyte	28.70	8.75	14.19	39.84	15.57	32.85

The CVs of $LiCoO_2$|GPE|graphite coin cells were examined to further explain the performance difference of PVA-CN based polymer LIBs with different formation technologies. When the battery is subjected to CV test before the gelation of PVA-CN, it is seen from **Fig. 6**b that the current in the 1st CV of 2.5–3.6 V is larger than that in the 2nd CV cycle, which can be attributed to the electrolyte reduction on the surface of graphite anode to form a SEI film[44]. Whereas, when the cell is subjected to CV test after the gelation of PVA-CN, the voltage range of SEI formation shrinks to 2.5–3.4 V (**Fig. 6**a). This phenomenon confirms that the pre-formed PVA-CN based gel hinders the reduction of liquid electrolyte and the construction of SEI film.

In addition, **Fig. 6**b shows that the 1st and 2nd CV curves are very similar to the 3rd to 5th curves, which indicates that when a SEI film is constructed on the electrode, the subsequent formation of PVA-CN based gel almost does not influences the reversibility and kinetics of electrode. However, when the cell is subjected to CV test after the gelation of PVA-CN, it is seen from **Fig. 6**a that the cell shows a much less cathodic current (from 3.7 V) and an obviously higher cathodic peak voltage, which suggests an apparently lager polarization. The cathodic current gradually increases and the cathodic peak voltage gradually decreases with the increase of CV cycles, indicating that the unstable SEI film with high resistance is sequentially reconstructed during cycling. This confirms that the pre-formed PVA-CN based gel hinders the construction of SEI film with high conductivity during cell formation.

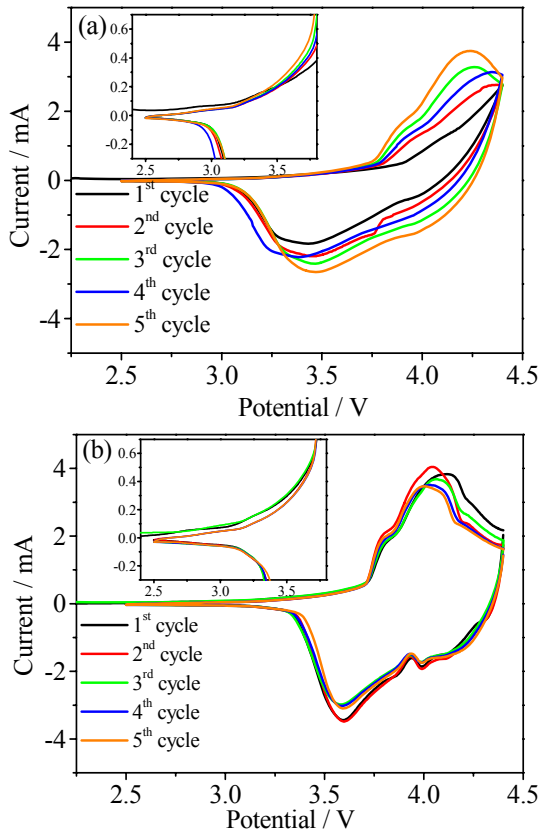

Fig. 6. CVs of CR2032 type $LiCoO_2$|GPE|graphite cells with Technology 1 (a) and Technology 2 (b) at a scan rate of 0.1 mV s^{-1}.

Moreover, the potential gap between anodic and cathodic peak (△Ep) reflects the polarization degree of the electrode. It is found that the cell with Technology 2 shows a much less △Ep and an obviously larger peak current than cell with Technology 1, indicating a considerably less polarization of former cells. These results are well consistent with the electrochemical performance results shown in **Fig. 5**. The formation technology is significant for the fabrication of a better electrode/ GPE interface and the improvement of electrochemical performance for GPE type battery. The formation process should be completed in a liquid phase to ensure a stable SEI film formed on the electrode with lower resistance and high ionic conductivity.

Conclusions

In this work, we investigated the in-situ gelation mechanism of the novel PVA-CN based GPE and optimized the electrode/GPE interface in $LiCoO_2$|GPE|graphite batteries. The polymerization of PVA-CN is initiated by the PF_5 and a trace of water in $LiPF_6$ based electrolyte solution. The gel reaction of PVA-CN in battery is best to be completed after the battery formation, which is found to be an effective way to fabricate an electrode/electrolyte interface with less resistance and improve the electrochemical performance of GPE type batteries. These novel mechanism and interface optimization technology can provide a new way for the design, preparation and application of novel cyano electrolyte materials for LIBs with high electrochemical and safety performance, which can also be applied to other chemical power sources using GPEs prepared by in-situ thermal polymerization, such as lithium sulphur battery, dye-sensitized solar cell and supercapacitor.

Acknowledgements. We thank Dongguan ADF battery Co., Ltd for providing testing battery cores. This work was supported by National Key Basic Research Program of China (No. 2014CB932400), National Natural Science Foundation of China (No. 51072131, 51202121 and 51232005), the Key Project for Basic Research for three main areas of Shenzhen (No. JC201104210152A), Guangdong Province Innovation R&D Team Plan for Energy and Environmental Materials (No. 2009010025) and Shenzhen Technical Plan Project (No. JCYJ20120831165730900).

References

1. N. S. Choi, Z. Chen, S. A. Freunberger, X. Ji, Y. K. Sun, K. Amine, G. Yushin, L. F. Nazar, J. Cho and P. G. Bruce, Angew. Chem. Int. Ed., 2012, 51, 9994-10024.
2. G. Jeong, Y. U. Kim, H. Kim, Y. J. Kim and H. J. Sohn, Energy Environ. Sci., 2011, 4, 1986-2002.
3. R. Bouchet, S. Maria, R. Meziane, A. Aboulaich, L. Lienafa, J. P. Bonnet, T. N. Phan, D. Bertin, D. Gigmes and D. Devaux, Nat. Mater., 2013, 12, 452-457.
4. N. Kamaya, K. Homma, Y. Yamakawa, M. Hirayama, R. Kanno, M. Yonemura, T. Kamiyama, Y. Kato, S. Hama and K. Kawamoto, Nat. Mater., 2011, 10, 682-686.
5. W. Huang, Z. Zhu, L. Wang, S. Wang, H. Li, Z. Tao, J. Shi, L. Guan and J. Chen, Angew. Chem., 2013, 125, 9332-9336.
6. Y. Zhu, S. Xiao, Y. Shi, Y. Yang, Y. Hou and Y. Wu, Adv. Energy Mater., 2014, 4, 1-9.
7. H. Fan, H. Li, L. Z. Fan and Q. Shi, J. Power Sources, 2014, 249, 392-396.
8. P. Isken, M. Winter, S. Passerini and A. Lex Balducci, J. Power Sources, 2013, 225, 157-162.
9. W. C. Kang, H. G. Park, K. C. Kim and S. W. Ryu, Electrochim. Acta, 2009, 54, 4540-4544.
10. H. Li, X.T. Ma, J. L. Shi, Z. K. Yao, B. K. Zhu and L. P. Zhu, Electrochim. Acta, 2011, 56, 2641-2647.
11. S. I. Kim, H. S. Kim, S. H. Na, S. I. Moon, Y. J. Kim and N. J. Jo, Electrochim. Acta, 2004, 50, 317-321.
12. S. H. Kim, K. H. Choi, S. J. Cho, E. H. Kil and S. Y. Lee, J. Mater. Chem. A, 2013, 1, 4949-4955.
13. S. S. Hwang, C. G. Cho and H. Kim, Electrochem. Commun., 2010, 12, 916-919.
14. H.S. Kim and S. I. Moon, J. Power Sources, 2005, 146, 584-588.
15. J. Choi, J. H. Yoo, W. Y. Yoon and D. W. Kim, Electrochim. Acta, 2014, 132, 1-6.
16. J. R. Nair, C. Gerbaldi, M. Destro, R. Bongiovanni and N. Penazzi, React. Funct. Polym., 2011, 71, 409-416.
17. Y. Zhou, S. Xie, X. Ge, C. Chen and K. Amine, J. Appl. Electrochem., 2004, 34, 1119-1125.
18. D. Zhou, L. Z. Fan, H. Fan and Q. Shi, Electrochim. Acta, 2013, 89, 334-338.
19. S. S. Zhang, J. Power Sources, 2006, 162, 1379-1394.
20. Y. S. Kim, Y. G. Cho, D. Odkhuu, N. Park and H. K. Song, Sci. Rep., 2013, 3.
21. K. Xu, Chem. Rev., 2004, 104, 4303-4418.
22. J. S. Shin, C. H. Han, U. H. Jung, S. I. Lee, H. J. Kim and K. Kim, J. Power Sources, 2002, 109, 47-52.
23. D. Wöuhrle and G. Knothe, J. Polym. Sci. Part A, 1988, 26, 2435-2447.

24. M. Lu, Y. Wei, B. Xu, C. F. C. Cheung, Z. Peng and D. R. Powell, Angew. Chem. Int. Ed., 2002, 41, 1566-1568.
25. X. Li, S. Goh, Y. Lai and S. M. Deng, J. Appl. Polym. Sci., 1999, 73, 2771-2777.
26. H. X. Yu, H. Cui and J. B. Guan, Luminescence, 2006, 21, 81-89.
27. T. Takahagi, I. Shimada, M. Fukuhara, K. Morita and A. Ishitani, J. Polym. Sci. Part A, 1986, 24, 3101-3107.
28. N. Inagaki, S. Tasaka and Y. Yamada, J. Polym. Sci., Part A, 1992, 30, 2003-2010.
29. B. V. Crist, Surf. Sci. Spectra, 1992, 1, 376-380.
30. G. Beamson and D. Briggs, Wiley, 1992.
31. J. M. Burkstrand, J. Vac. Sci. Technol., 1979, 16, 363-365.
32. Y. Okamoto, J. Electrochem. Soc., 2013, 160, A404-A409.
33. V. Kabanov, V. Zubov, V. Kovaleva and V. Kargin, J. Polym. Sci. Part C, 1963, 4, 1009-1026.
34. E. Oikawa and S. Kambara, J. Polym. Sci. Part B, 1964, 2, 649-653.
35. K. H. Lee, H. S. Lim and J. H. Wang, J. Power Sources, 2005, 139, 284-288.
36. F. Nobili, R. Tossici, F. Croce, B. Scrosati and R. Marassi, J. Power Sources, 2001, 94, 238-241.
37. F. Croce, F. Nobili, A. Deptula, W. Lada, R. Tossici, A. D. Epifanio, B. Scrosati and R. Marassi, Electrochem. Commun., 1999, 1, 605-608.
38. M. Umeda, K. Dokko, Y. Fujita, M. Mohamedi, I. Uchida and J. Selman, Electrochim. Acta, 2001, 47, 885-890.
39. G. T. K. Fey, W. H. Yo and Y. C. Chang, J. Power Sources, 2002, 105, 82-86.
40. Y. B. He, Z. Y. Tang, Q. S. Song, H. Xie, Y. G. Liu and Q. Xu, J. Electrochem. soc., 2008, 155, A481-A487.
41. S. Prabakar, Y. H. Hwang, E. G. Bae, S. Shim, D. Kim, M. S. Lah, K. S. Sohn and M. Pyo, Adv. Mater., 2013, 25, 3307-3312.
42. K. Yang, L. Z. Fan, J. Guo and X. Qu, Electrochim. Acta, 2012, 63, 363-368.
43. S. S. Zhang, J. Power Sources, 2007, 164, 351-364.
44. Y. B. He, B. Li, Q. H. Yang, H. Du, F. Kang, G. W. Ling and Z. Y. Tang, J. Solid State Electrochem., 2011, 15, 1977-1985.

Table of Contents Entry

Investigation of cyano resin based gel polymer electrolyte: in-situ gelation mechanism and electrode/electrolyte interfacial fabrication in lithium-ion battery

Dong Zhou,[a,b] Yan-Bing He,[a] Qiang Cai,[b] Xianying Qin,[a] Baohua Li,[a] Hongda Du,[a] Quan-Hong Yang[a] and Feiyu Kang[a,b]*

[a] *Engineering Laboratory for the Next Generation Power and Energy Storage Batteries, and Engineering Laboratory for Functionalized Carbon Materials, Graduate School at Shenzhen, Tsinghua University, Shenzhen 518055, China, fykang@mail.tsinghua.edu.cn*

[b] *Laboratory of Advanced Materials, School of Materials Science and Engineering, Tsinghua University, Beijing 100084, China*

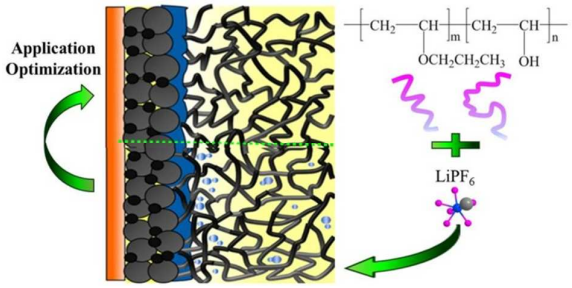

This paper reports the gelation mechanism of PVA-CN based GPE and fabricate an electrode/GPE interface with less resistance during formation.